



PERGAMON

Quaternary Science Reviews 22 (2003) 371–385



Determining paleoceanographic circulations, with emphasis on the Last Glacial Maximum

Carl Wunsch*

Department of Earth, Atmospheric and Planetary Sciences, Massachusetts Institute of Technology, 54-1520, 77 Massachusetts Ave, Cambridge, MA 02139, USA

Received 3 May 2002; accepted 15 August 2002

Abstract

The inference, from radiocarbon and other data, that the North Atlantic Ocean circulation during the Last Glacial Maximum was reduced, is examined. Because glacial periods are thought to be windier than non-glacial ones, a reduced circulation is difficult to rationalize. A first step is to note that the circulation of mass is unlikely to correspond simply to the circulation of heat or freshwater (salt). By merely permitting an enhanced input of southern hemisphere water into the North Atlantic, one can accommodate significantly increased radiocarbon ages. Such an input is equally interpretable as owing to an increased mass circulation, rather than a decreased one. Inferred estimates from paleo-shear estimates in the Florida Current are re-interpreted as producing an indeterminate net flow there. Determination of the paleocirculation rates is not simpler than the problem in the modern ocean: it is fully three-dimensional and requires an adequate data base to determine the mass flux rates.

© 2002 Elsevier Science Ltd. All rights reserved.

1. Introduction

Determination of the circulation of the ocean as it exists today has taken an effort extending over 100 years, culminating most recently with the very large World Ocean Circulation Experiment (WOCE). Using satellite data, detailed ship-board surveys, and tens of thousands of in situ measurements combined with the most complex general circulation models that can be accommodated by the largest computers, we have made a quantitative estimate of the oceanic state, and its variability. Nonetheless, despite the best efforts of thousands of people and the investment of hundreds of millions of dollars, there remain serious uncertainties about the present oceanic state and the extent to which, and how it is changing.

When it comes to understanding past (and future) climate, an issue of major concern is the determination of the ocean circulation in various geological periods. The purpose of this paper is to re-examine this question in light of what has been learned about the determination of the modern circulation, and how it is to be interpreted. A main goal is to separate inferences clearly

demanding by the observations from those that are assumptions—plausible or otherwise. Only by such separation can one design observational programs to address areas of prime ignorance. To make the discussion manageable, I will focus specifically on the circulation during the Last Glacial Maximum (LGM), but the fundamental issues will not be different in any other period preceding the instrumental record.

One of the more surprising deductions about the oceanic circulation in the North Atlantic during the LGM is that it was generally more sluggish than it is today. Perhaps the most specific statement comes from the conclusion by Lynch-Stieglitz et al. (1999) that the geostrophic shear in the Florida Straits diminished, and therefore that the “thermohaline circulation” was reduced. Although as summarized by Boyle (1995), little is clear about what happened in the North Atlantic during the LGM, there was an apparent shift in the properties and depth of North Atlantic Deep Water (NADW), and available radiocarbon ages appeared to have doubled (Broecker et al., 1990). Taken together, there is a widespread, if not universal, belief that the LGM circulation was weaker than today.

Contrary inferences have indeed been published: Legrand and Wunsch (1995) showed that $\delta^{13}\text{C}$ and other tracers were consistent with a circulation strength

*Tel.: +1-617-253-5937; fax: +1-617-253-4464.

E-mail address: cwunsch@mit.edu (C. Wunsch).

unchanged from today (but consistent also with any circulation magnitude). Yu et al. (1996) described protactinium/thorium ($^{231}\text{Pa}/^{230}\text{Th}$) data requiring an unchanged or increased export from North Atlantic during the LGM.

Taken at face value, any inference of a reduced circulation is surprising, in view of another widespread conclusion—the wind system over the globe intensified during the LGM. This conclusion is drawn primarily from dust deposits in cores, and is a straightforward inference about a world in which the atmospheric surface thermal gradient from pole to equator was increased—leading to a strengthening of the zonal wind systems (e.g., Crowley and North, 1991). Increased aridity may also have contributed to larger rates of dust deposition, but the primary deduction of stronger surface winds is difficult to avoid. Today, the intensity of the general circulation of the ocean is primarily a function of the wind-strength. All of the elements determining the large-scale flow (Ekman layers, western boundary current intensities, equatorial undercurrents, etc.) are directly proportional to the wind-stress, τ , and its curl. Increases in current intensities would generally strengthen other elements of the circulation, such as the eddy field, that are dependent upon large-scale instabilities.

What may be less widely understood however, is that mixing rates during the LGM were probably also strengthened—for two distinct reasons (Munk and Wunsch, 1998). First, much of the deep ocean turbulence permitting the cold dense water to mix vertically across the stable abyssal stratification comes from the wind field; a strengthened wind field would be expected to amplify the mixing rates. Second, a significant fraction of the abyssal turbulence is now thought to originate with tidal forcing. During the LGM, sealevel was more than 120 m lower than today. Such a lowered sealevel removes the highly dissipative continental shelves from the system, potentially greatly increasing the deep ocean tidal amplitudes (to be certain, a model is required) and hence the abyssal mixing rates. Although one cannot categorically rule out some unexpected structure in the LGM wind field or tidal mixing leading to a weakened North Atlantic flow, Occam's razor leads one to anticipate a strengthening of the ocean mass circulation during the LGM, although the details are unknown.

At this point, it is necessary to make the elementary observation that there are many ocean circulations: those for mass, temperature, salt, oxygen, etc., and that they are all different. The general circulation of mass need not even qualitatively resemble the circulation of a scalar property carried by the circulation. In the modern system, the very different patterns of mass, temperature, salt, oxygen and nutrient circulation in the Atlantic Ocean are examples (Ganachaud and Wunsch, 2000,

2002); the modern North Atlantic Ocean imports heat on the average, but exports oxygen and nitrate. *None of the scalar fluxes resembles the pattern of mass transport in any simple way.*

Unfortunately, common terminology has obscured the necessity of distinguishing the circulations of varying properties. For example, consider the following statement in a recent textbook (Bradley, 1999, p. 254):

Circulation of water at the ocean surface is largely a response to the overlying atmospheric circulation which exerts drag at the surface. However, circulation of deeper waters in the oceans of the world is a consequence of density variations, which result from differences in temperature and salinity brought about by sensible and latent heat fluxes, precipitation, and runoff at the ocean surface; this is termed the thermohaline circulation.

From this passage, one would never suspect that the density contrasts of the more obviously wind-driven circulation are *much* larger than those of the abyssal circulation. Indeed, these density contrasts are used in both the classical dynamical and inverse methods to infer the upper (and abyssal) ocean circulation. The directly buoyancy-driven circulation is sometimes called the Goldsbrough or Stommel-Goldsbrough circulation (Huang and Schmitt, 1993), and is an order of magnitude weaker than the wind-driven component.

The abyssal mass circulation, which is often mislabeled as the “thermohaline” circulation, is essentially wind-driven with a major contribution from tidal forcing (Munk and Wunsch, 1998). Buoyancy forces acting at the seasurface are very ineffective in *driving* an abyssal circulation. The essential argument is an energetic one: surface buoyancy forcing is not capable of doing significant amounts of work on the fluid, and hence there is little circulation “forced” by transfers of heat and moisture. As described by Munk and Wunsch (1998), Huang (1999) and others, the energy argument is equivalent to the thermodynamic one embodied in “Sandström's Theorem” and implies that the circulation must be primarily mechanically driven (Paparella and Young, 2002 provide a fluid-dynamical argument). To lift fluid across the deep stratification, a fundamentally turbulent process is required, one sustained by an external source of energy. The actual thermohaline circulation, literally the movement of heat and salt, is dominated by the direct wind-forcing, in which the gyre circulation at the surface, e.g., the Gulf Stream, Kuroshio, and the intensity of deep turbulent mixing determine the overall rates. Spatial variations in density at depth do not drive the circulation; indeed with the circulation in near-geostrophic balance, one can infer neither that the pressure field drives the flow nor that the flow drives the pressure field: they represent a balanced system. The geostrophic relationship does permit one to

use the density field to calculate (diagnostically) important aspects of the flow field, but one is not entitled to infer that the density field drives the circulation anymore than one can do so in the upper ocean.

The terminology “thermohaline circulation” conflates the circulations of mass, heat and salt into one, but in the modern system, these are very different, having disparate surface boundary conditions (see the reviews by Bryden and Imawaki, 2001; Wijffels et al., 2001). In the wider literature, several inconsistent definitions exist:

- (1) The circulation of mass, heat and salt (although these all differ),
- (2) The ‘abyssal’ circulation,
- (3) The meridional overturning circulation,
- (4) The ‘conveyor’ (itself with various inconsistent definitions),
- (5) The circulation driven by surface buoyancy forcing,
- (6) The circulation driven by deep density and/or pressure differences,
- (7) Net ocean basin property export, such as protactinium from the North Atlantic.

Stommel (1961) apparently was the first to use the expression “thermohaline” for a circulation controlled by surface buoyancy forces. But he explicitly included mechanical stirring in his conceptual model, as required to homogenize his box reservoirs; this model element was conveniently ignored by many succeeding investigations and it is unclear whether box models without explicit mechanical forcing can be physically realized. Furthermore, in a comparatively little noticed paper, Stommel and Rooth (1968) showed that the inclusion of wind-stress completely changed the stability properties of a thermally driven system.

Surface exchanges of heat and fresh water with the atmosphere do set the properties with which fluid reaches mid-depths or the seafloor, after sometimes intense entrainment and detrainment exchanges with the ambient fluid, and thus control, in part, the net transfer of heat and salt. The modern system strongly supports the supposition however, that one could have a strengthened mass circulation with a simultaneously reduced heat flux. One must attempt to understand what is really determined by the data, and what is simply hypothesis.

With a few exceptions, almost all direct inferences about paleocirculations are based upon measurements of the apparent distributions of various passive scalar tracers in the fluid ocean. By “passive”, is here meant properties not influencing the fluid density. As Legrand and Wunsch (1995) pointed out, if the tracers are stable, or have unknown sources and sinks, such distributions by themselves provide no information about the rates of oceanic mass flux. Water mass volumes are not indicators of either flow or transformation values. They

concluded that only scalar properties accompanied by known rates of production or consumption could begin to constrain the flow magnitudes. An oxygen distribution with known utilization or production rates as a function of position would be one possibility. But the most obvious candidates were, and continue to be, radiocarbon or uranium/thorium series distributions, with the rate “clock” being controlled by the known decay times.

The intention here is to examine the possibilities for determining the mass circulation during the LGM using radiocarbon and similar age distributions. The analysis becomes a vehicle for a general discussion of tracer ages and their information content. At the end, we will briefly touch on the line of evidence based upon paleogeostrophic shear estimates.

2. A simple North Atlantic model

To be specific, we will use a simple steady 18-box model of the North Atlantic Ocean chosen to have some zero-order realism, but no realistic detail. The model has a surface layer of 100 m thickness, a “thermocline” layer of 1000 m thickness, and an abyss of 4000 m thickness. There is a western boundary current region and an interior, as well as nominal subpolar, subtropical and equatorial regions (see Fig. 1). Mass transfers between the boxes are represented as $J_{ij} > 0$, being the net mass flux from box i to neighbor j ; the general structure is described by Wunsch (1988a), who connects the J_{ij} and tracer concentrations to conventional advection and mixing processes. The model is meant to capture the essential spatial features of the general circulation: separate western boundary current and interior areas, and surface, thermocline and abyssal vertical structures. Inclusion of other features, e.g. the two basins on either side of the Mid-Atlantic Ridge, would also be desirable but these are probably secondary to the features included. Existence of the three-dimensional structure rather than its detail is required. The model is simpler in the zonal direction than that of Legrand and Wunsch (1995), but does occupy the full water column. An advantage of this formalism is that noisy property gradients need not be explicitly computed, although they are present implicitly.

The values of J_{ij} are chosen to give a rough sense of the actual North Atlantic mass fluxes. So for example, there is a “Gulf Stream” carrying 40 Sv north (10 of that is in the surface layer), a deep western boundary current at 20 Sv, and a “convective” region in the north of 15 Sv. These numbers are only rough order of magnitude values, and some of the inter-box exchanges are left at zero. Numerical changes will modify the results in detail, but not in gross character. Given the J_{ij} , one writes the corresponding transfer of any scalar property, C_p , as

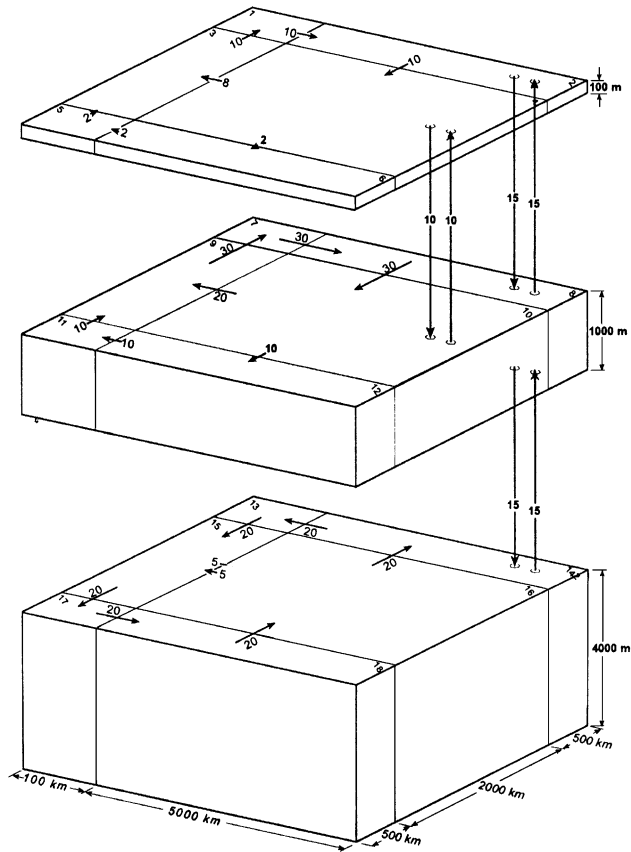


Fig. 1. Three-dimensional box model with exchanges, J_{ij} given in Sverdrups. Small numbers are the box label.

$C_{pi}J_{ij}$, and the property change in box i with a discrete time step Δt is

$$C_{pi}(t + \Delta t) - C_{pi}(t) = - \sum_{j \in N_i} J_{ij} \frac{\Delta t}{V_i} C_{pi}(t) - \lambda_p \frac{\Delta t}{V_i} C_{pi}(t) + \sum_{j \in N_i} J_{ji} \frac{\Delta t}{V_i} C_{pi}(t) + q_i(t). \quad (1)$$

Here, V_i is the volume of box i , $q_i(t)$ is any externally imposed source or sink of C_{pi} and $j \in N_i$ denotes the indices of the neighboring boxes to i (a maximum of six). λ_p is the decay time-constant for C_p , e.g., 1/8500 year for radiocarbon (^{14}C). This expression is intended as a quantitatively useful discrete analog to the ordinary advection/diffusion/decay equation:

$$\frac{\partial C_p}{\partial t} + \mathbf{v} \cdot \nabla C_p = \nabla(\mathbf{K} \nabla C_p) - \lambda_p C_p + q, \quad (2)$$

where \mathbf{K} is the mixing tensor. Energetics per se, of the J_{ij} , are not the concern here, only the extent to which we can make inferences about them from their influence on tracers.

Choosing time in units so that $\Delta t = 1$, and making vectors

$$\mathbf{x}(t) = [C_{p1}(t), C_{p2}(t), \dots, C_{pM}(t)]^T,$$

$$\mathbf{q}_p(t) = [q_{p1}(t), q_{p2}(t), \dots, q_{pM}(t)]^T,$$

Eq. (1) is readily written in the canonical form:

$$\mathbf{x}_p(t + 1) - \mathbf{A}_p \mathbf{x}_p(t) + \mathbf{q}_p(t), \quad (3)$$

where \mathbf{A}_p is the state transition matrix (see Wunsch, 1988a for details), with,

$$A_{pii} = 1 - \sum_{j \in N_i} J_{ij} \frac{\Delta t}{V_i} - \lambda_p \Delta t, \quad (4)$$

$$A_{pij} = \sum_{j \in N_i} J_{ji} \frac{\Delta t}{V_i}, \quad j \neq i. \quad (5)$$

There are $M = 18$ boxes, with six in each layer as depicted. The structures of \mathbf{A}_p and $\mathbf{q}_p(t)$ determine the boundary conditions being applied. If row i of \mathbf{A}_p is set to zero, then $x_i(t) = q_{pi}(t)$ and one has a concentration boundary condition in box i ; otherwise, $q_{pi}(t) \neq 0$ implies a flux boundary value $q'_i(t)$, such that

$$q_{pi}(t) = q'_i(t) \Delta t / V_i(t). \quad (6)$$

Eq. (3) represents the “parent” tracer; the stable “daughter” tracer, C_d , into which it decays satisfies a partial differential equation of form:

$$\frac{\partial C_d}{\partial t} + \mathbf{v} \cdot \nabla C_d = \nabla(\mathbf{K} \nabla C_d) + \lambda_p C_p. \quad (7)$$

In the present discrete form:

$$\mathbf{x}_d(t + 1) = \mathbf{A}_d \mathbf{x}_d(t) + \lambda_p \mathbf{x}_p(t), \quad (8)$$

with $\mathbf{x}_d(t) = [C_{d1}(t), C_{d2}(t), \dots, C_{dM}(t)]^T$,

$$A_{dii} = 1 - \sum_{j \in N_i} J_{ij} \frac{\Delta t}{V_i}, \quad (9)$$

$$A_{dij} = \sum_{j \in N_i} J_{ji} \frac{\Delta t}{V_i}, \quad j \neq i. \quad (10)$$

At least two working definitions of tracer “age” for a water mass exist. One (e.g., Jenkins, 1988),

$$\tau_p(t, \lambda_p) = \frac{1}{\lambda_p} \ln \left(1 + \frac{[C_d(t)]}{[C_p(t)]} \right), \quad (11)$$

involves the ratio of the measured parent/daughter concentrations. This definition is used for tritium-helium-3 ($^3\text{H}/^3\text{He}$), $\lambda_{^3\text{H}} = 1/17.9$ year, and several other pairs. There is however, a quite different common definition,

$$\tau'_p(t, \lambda_p) = - \frac{1}{\lambda_p} \ln \left[\frac{C_p(z)}{C_p(0)} \right], \quad (12)$$

involving only the parent, referred to the surface (or other reservoir) value. This definition is commonly used for radiocarbon, because the daughter product, ^{14}N , is not measured. For a solid body or a fluid without mixing, $\tau_p = \tau'_p$. Unfortunately, in real fluids, the two definitions can produce ages differing by more than an order of magnitude (see Appendix A), supporting the inference (Wunsch, 2002) that tracer ages are not fundamental fluid flow properties.

The interpretation of τ_p becomes very complex because, as the ratio of two tracers each satisfying a linear partial differential equation with its own boundary conditions, it satisfies a very complicated non-linear partial differential equation (e.g., Jenkins, 1988; Wunsch, 2002) although it is readily computed from the coupled linear system (3, 8, boundary conditions, and the definition 11). In contrast, τ'_p is determined from (2) and its boundary conditions alone. Great care is thus required for the interpretation of ages. (^{14}C is usually reported as $\Delta^{14}\text{C}$, relative to a reference standard and accounting for fractionation effects; this distinction will be ignored here.) τ_p will be used for most theoretical age calculations, with the pretence that ^{14}N can be measured, both because it is used for the $^3\text{H}/^3\text{He}$ pair, and because it seems less arbitrary than the assumption that the local surface reservoir age is the appropriate reference value. All calculations can be readily done using τ'_p , resulting in no qualitative change. A brief comparison of the transient behavior of the two ages is provided later.

3. Time constants

Knowledge of the time scales over which the ocean responds to external disturbances are necessary for

understanding the ocean circulation, and particularly important for explaining climate change. A variety of time scales is usually quoted for the ocean. The radiocarbon ages of the ocean are longer than 1000 years in the northeast Pacific, and are a few hundred years in the North Atlantic (correcting for the finite age of the surface waters). These numbers, particularly the North Pacific values, are treacherous because they are often interpreted as being the time since the water was at the seasurface; but because surface water does not necessarily equilibrate its carbon content with the atmosphere (Broecker and Peng, 1982) and because the ocean mixes, no such simple interpretation can be made. (Age calculations from observations are discussed by Jenkins, 1988, Gray and Haine, 2001, Wunsch, 2002, etc.)

A more straightforward time scale can be obtained by dividing the global ocean volume by the approximate rate of bottom water formation, $T \approx 1.4 \times 10^{19} \text{ m}^3 / 30 \times 10^6 \text{ m}^3/\text{s} \approx 1500$ years, as the time to completely replace all of the volume. Such a time scale is misleading in that parts of the ocean are flushed much more quickly (e.g., tracers move from the seasurface to the seafloor in less than a decade), and large volumes of ocean are replaced on time scales far shorter than 1500 years, with others probably not fully mixed for

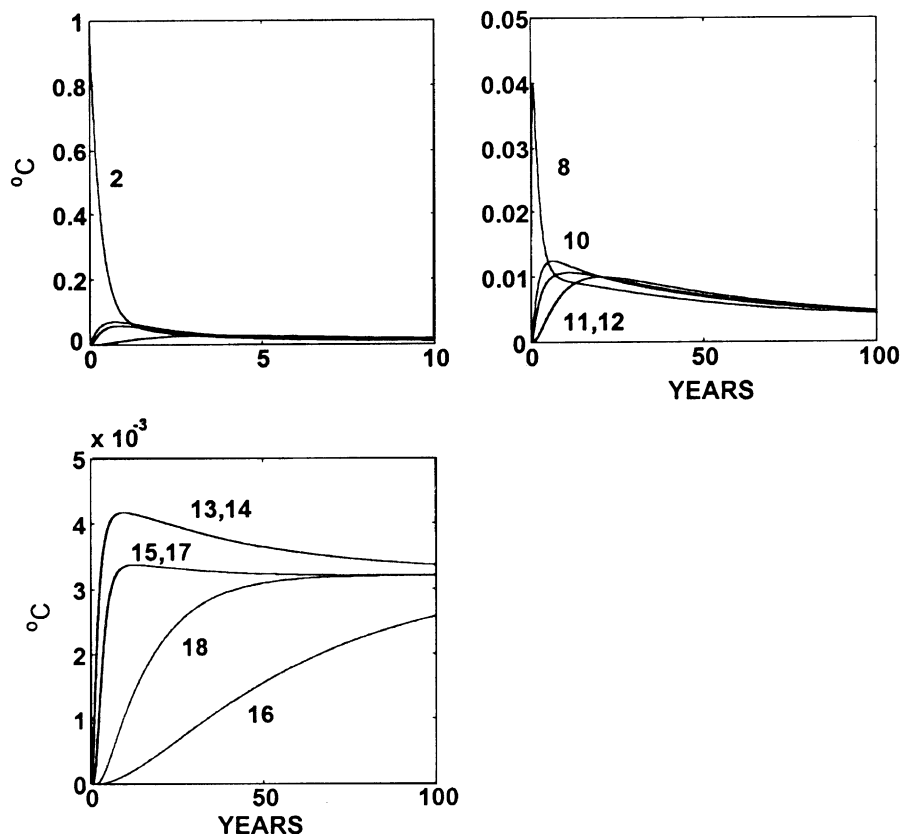


Fig. 2. Green function for a stable tracer introduced as a concentration boundary condition in box 2. Box numbers label each curve. Note that for upper level, the time scale is much expanded to show the initial transient.

much longer times. But the number suggests that the ocean has some partial memory extending back to well over 1000 years—a very serious complication in the interpretation of both modern and paleo-climate states.

To understand the way the North Atlantic responds to external tracer forcing, consider first a stable tracer, C , with $\lambda_p = 0$. For the moment, the system is assumed closed on all boundaries except the surface. Let the tracer concentration in box 2 be set to 1 for one time step, and then restored to zero. The subsequent evolution of the tracer field is part of what is usually called the numerical Green function for the problem. The result is shown in Fig. 2. Evidently, about 200 years are required for the abyss to reach its final asymptote of a uniform concentration. But different regions of the model undergo transients with different time scales. The complete numerical Green function is built up by carrying out the identical experiment, with each box in turn being the region of the imposed initial perturbation, but we will not display the full result here. Green functions were used by Wunsch (1988a), Mémary and Wunsch (1990); Gray and Haine (2001) and others to formulate and solve tracer inverse problems.

Extrapolating these results globally is difficult without a global model, but one might be nervous about conclusions that the ocean is well mixed (that is has equilibrium distributions) on time scales less than 1000 years, as is sometimes claimed.

A more formal determination of system time constants can be obtained by finding the eigenvectors of the system and their associated eigenvalues, which are the time constants of the system. These results, while important, have been placed in Appendix B. The time constants of the system eigenvectors (which are *not* orthogonal) range from less than 1 year to about 50 years, with one eigenvalue corresponding to an infinite time scale—reflecting the infinite residence time of a closed system with a stable tracer.

4. Ages

Consider first the $^3\text{H}/^3\text{He}$ -like system, with a half-life for tritium of about 12.5 years. The analysis in Appendix B now produces a maximum time constant of $1/\lambda_{\text{tritium}} = 17.86$ years with the asymptotic state for any Green function now being zero. For greater simplicity of interpretation, ^3H is imposed as a fixed concentration $C_p(z=0) = 1$ (not time-dependent), in all six surface boxes and held at that value subsequently. The resulting “Heaviside function” response will have no time scales present other than those internal to the model. For ^3He , we set $C_d(z=0) = 0$, to represent instantaneous outgassing. With a constant surface tritium value, the system asymptotes to a steady-state, as depicted in Figs. 3 and 4.

Tritium–helium ages for the entire domain lie between about 30 and 75 years in the abyss, but it takes nearly

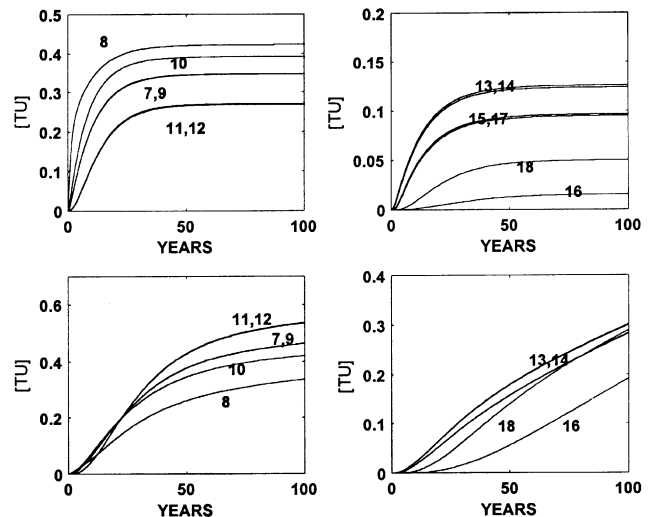


Fig. 3. Response to a fixed tritium-like concentration in boxes 1–6, held at 1 TU until a nearly steady-state is achieved. Box numbers show the response as a function of position. Upper two panels are tritium concentrations, and lower two are the corresponding helium ones. Surface reservoir age is zero here.

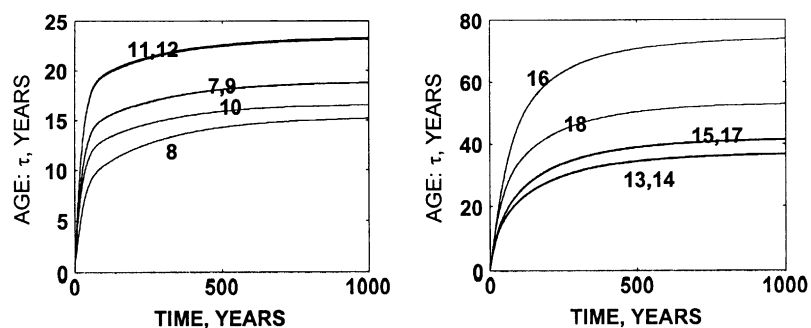


Fig. 4. Tritium–helium ages corresponding to Fig. 3. Notice the different time scales used for plotting the concentrations and ages τ . Some of the latter still have not reached their asymptotes after 500 years.

500 years to reach the asymptotes. This disparity of time scales is a symptom of the complexity of tracer ages.

5. Radiocarbon ages

We now focus on the radiocarbon age distribution of the model ocean, because it remains the most prominent of the tracer families now being used to infer rates of oceanic circulation in the LGM. The modern ocean is used as a point of comparison. The “ventilation” age is usually defined as the difference between the observed interior age, and that of the local surface value (although the deep value may be quite unrelated to the surface concentration). The surface reservoir (surface layer) of much of the modern North Atlantic Ocean has a nearly uniform radiocarbon age of about 400 years (Bard, 1988) as a result of buffering of the atmospheric input of radiocarbon, and the mixing with low radio-

carbon fluid from below. A surface concentration boundary condition is thus the most straightforward.

To begin, let us assume the basin is closed to the south with no contribution from the South Atlantic, and determine the $^{14}\text{C}/^{14}\text{N}$ distribution and the corresponding values of $\tau_{^{14}\text{C}}$, as depicted in Figs. 5 and 6. Approximately 1500 years is required to achieve a steady-state and in which the final ventilation ages of the deep water are only about 200 years, consistent with e.g., Broecker et al. (1991). In view of the discussion above however, it should be clear that 200 years is not any easily interpretable single time scale of the basin. Fifteen hundred years might perhaps be interpreted as a response time for achieving equilibrium of the abyssal ocean with the surface conditions, but such an equilibrium is unlikely ever to be achieved in practice—given the expected variations in surface $\Delta^{14}\text{C}$ and in the flow field over such a long time.

Even when computed from the same expressions involving the parent and daughter concentrations, the tracer ages for $^3\text{H}/^3\text{He}$, $^{14}\text{C}/^{12}\text{N}$ are radically different (compare Figs. 4 and 6). That tracer ages are not an intrinsic property of the fluid flow, but depend directly upon λ_p , was discussed in Wunsch (2002). Any tracer age in a single region of the model is a complex integral over the boundary condition time history, and involves directly the entire set of exchange rates J_{ij} , as well as λ_p ; no simple interpretation as the time since the fluid was at the surface exists. Because turbulent mixing is now generally believed extremely spatially inhomogeneous (e.g., Ledwell et al., 2000), it is not likely to be simply parameterized in terms of one or two globally useful numbers, and separating advection from mixing is unlikely to be possible with a coarsely resolved suite of tracers.

It is useful to compare the computation of $\tau_{^{14}\text{C}}$ with that of $\tau_{^3\text{H}}$. Because these are boundary value problems, it is apparent, without actually running the model that the solution will depend sensitively upon the boundary

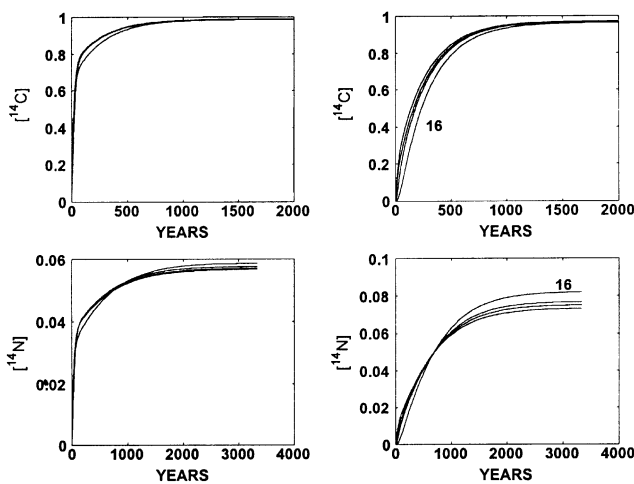


Fig. 5. Step response of the $^{14}\text{C}/^{14}\text{N}$ system analogous to that for $^3\text{H}/^3\text{He}$ except that a surface age of 400 years has been enforced.

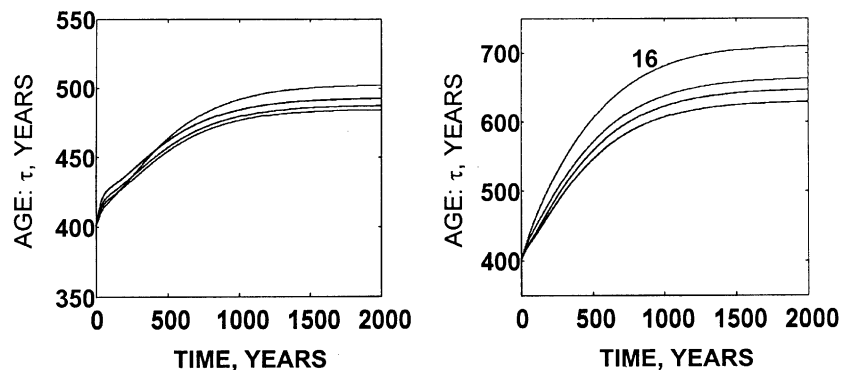


Fig. 6. The “ventilation” ages for the results in Fig. 5 computed as the difference between the in situ age and the surface ages are now about 200+ years, in contrast to the tritium–helium-3 ages. Note that lateral age gradients of order 100+ years exist in the abyss even after 2000 years of integration in the steady state.

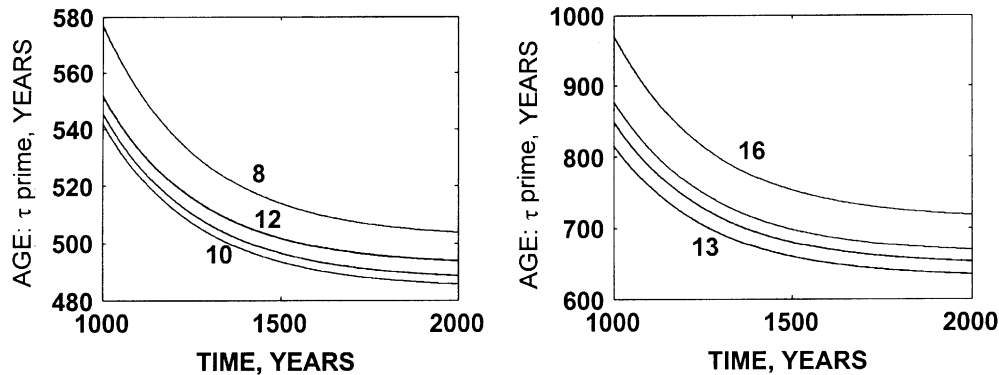


Fig. 7. Radiocarbon ages computed as τ'_{14C} from the parent distribution alone, with a surface concentration equivalent to an age of 400 years applied to the surface. Compare to Fig. 6. The earlier time history is a general decay from extremely large initial values when the concentrations of ^{14}C are very small everywhere except at the surface.

conditions of the problem. Fig. 7 displays the time history of the last 1000 years of τ'_{14C} , corresponding directly to Fig. 6, except that the surface concentration was reduced to a value of 0.9551 corresponding to a 400 years age relative to a concentration of 1. Although at the asymptotes, τ'_{14C} is within a factor of two of τ_{14C} , the time histories are completely different, and the comparison depends on when it is carried out.

During the LGM, observations suggest that ventilation times in the North Atlantic abyss appear to become somewhat greater (Broecker et al., 1990; Boyle, 1995) at about 650 years, compared to about 350 years today. In a closed North Atlantic, as in the above calculation, the only way to achieve these longer time scales would be to drastically reduce the values of J_{ij} . Results of such calculations (not shown) demonstrate that by simply multiplying J_{ij} by a small number, the age of the abyssal water can be increased arbitrarily (not a surprise).

A more likely explanation (e.g., Adkins et al., 1998) is that the fraction of waters coming from the Southern Ocean, with much higher values of τ_{14C} , increased in the North Atlantic. Waters of southern hemisphere origin in the North Atlantic today have a radiocarbon age of about 1400 years (e.g., Broecker et al., 1991) and it is easy to see that by introducing a larger input of water of southern origin into the system, the radiocarbon age can be made to greatly increase. As an example, the ^{14}N value in the abyssal southeastern box (no. 18) of the abyssal layer was forced to a value, relative to the evolving ^{14}C concentration, so that the tracer age there is fixed at 1400 years at year 1000 following integration without the southern hemisphere end member. The result is shown in Fig. 8; after about 200 years, an asymptote to a new apparent ventilation time closer to 700–1000 years is obtained in the abyss. The calculated time scale for the shift to occur is not unlike that observed, as a transient time, by Adkins et al. (1998). Of course, no mass circulation change has occurred; it is only the presence of the southern hemisphere water in a

boundary box that has made the difference; the net meridional fluxes of ^{14}N (or of $\Delta^{14}C$) would of course be changed significantly. The Green function for a disturbance in box 18 (not shown), displays an overall adjustment time to the system as a whole of about 200 years. Modification of end members can, unsurprisingly, make very large changes in distributions with no change in mass circulation. Note the strong gradients in the abyssal ventilation age, in some cases amounting to 300 years between boxes. Near the defining box boundaries, shifts in the edges of the water masses can clearly produce large changes in local ages without necessarily implying that any large-scale mass flux changes have occurred. During the transition periods, the inter-box concentration differences can be very much smaller than they are at equilibrium.

To study the effect of a circulation change, the model was run from zero concentration, with $\tau_{14C} = 1400$ fixed in box 18, and after 1000 years, all of the J_{ij} were multiplied by 1.5, producing a 50% increase in both circulation and mixing. The resulting age history is shown in Fig. 9, with ages being only modestly reduced.

The above simple calculations demonstrate several truisms: (1) A change in the concentration at the southern boundary condition (end-member) ultimately affects the entire system, whether or not the mass circulation itself changes. (2) Resident tracer concentrations reflect integrals over space and time, of products of the flux rates and mixing parameters with the boundary concentrations (end-members). Separating the cause of a change into a modification in one set of parameters (fluxes/mixing rates) from the other (changes in end-members), is not possible from measurements of the concentration distribution alone. (3) The time to achieve an equilibrium with a change in concentration boundary conditions can greatly exceed the apparent tracer ventilation time. (4) Apparent ventilation times are strongly dependent upon the tracer decay constants as the pathways by which tracer reaches a particular

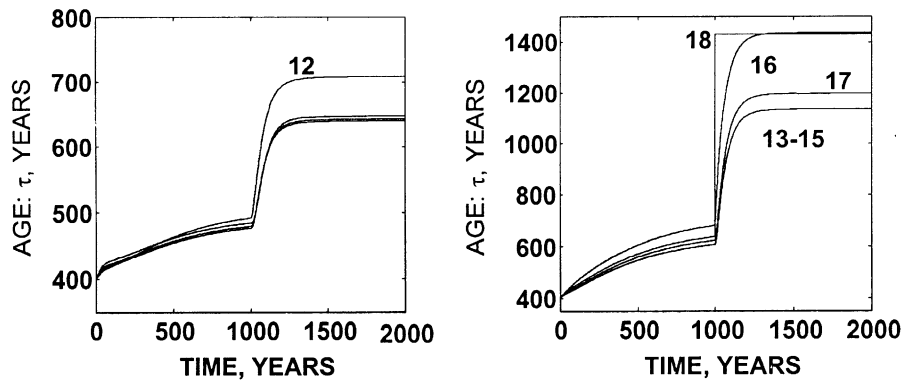


Fig. 8. Radiocarbon age in the same situation as in Fig. 6, except that the tracer age is forced to about 1400 years in the southeastern-most box after $t = 1000$ years, but with the mass flux otherwise unchanged. It takes about 200 years for the abyssal ventilation ages to reach 700 years and longer.

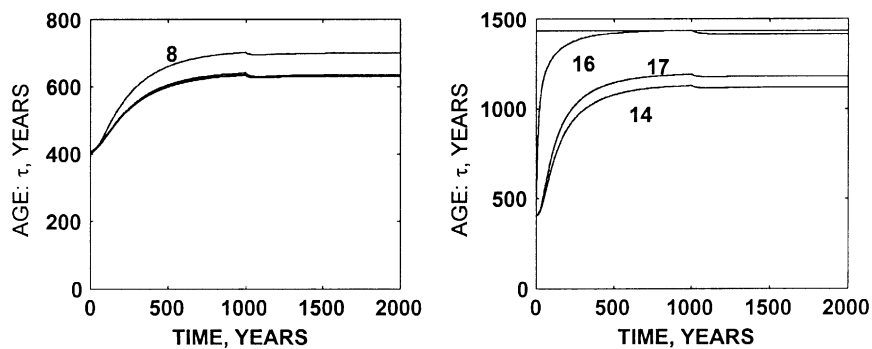


Fig. 9. Radiocarbon ages when the circulation is multiplied by a constant factor of 1.5 at $t = 1000$ years. The resulting ages (or corresponding ^{14}C concentrations) are only slightly changed.

position can be very different for tracers with different λ_p .

Because of the regional nature of the present interpretation, there is a large-degree of arbitrariness possible owing to the unknown open ocean boundary conditions. To become definitive, such models must become global. For example, a referee (R. Toggweiler) has suggested that apparently greater radiocarbon ages for deep southwestern Pacific water (e.g., Sikes et al., 2000) would be a problem for the present model. But there are many ways to lengthen radiocarbon ages generally. If one takes the simplest possible one-dimensional radiocarbon distributions subject to a steady-state vertical advective/diffusive balance (e.g., Appendix A and Wunsch, 2002), the radiocarbon age τ'_p relative to the surface water, depends directly upon the ratio of w/κ . By postulating differing dependencies of w , κ on an increased wind-speed, one can shift the radiocarbon age up or down. (τ'_p increases with increasing w/κ in this simple case). More generally, as we have seen, ages are the result of complex integrals of the space/time paths. If an increased windstress should lead fluid particles to spend more time circulating through the Southern Ocean before penetrating the Pacific, and/or having a greater disequilibrium with the atmosphere (greater ice cover in the ocean?) upon

encountering the surface there, one could readily increase the overall abyssal radiocarbon ages. Undoubtedly there are other means as well. The presence of water masses with greater ages in the Southern Ocean makes it even easier to increase the ages in the North Atlantic through modest mass flux shifts.

To understand the extent to which tracer concentrations can be used to infer the mass circulation requires consideration of the formal inverse problem.

6. The inverse problem

One can define an infinite number of inverse problems for a given “forward” or “direct” problem. Wunsch (1988a) and Mémerly and Wunsch (1990) chose to infer surface boundary conditions from observed interior distributions. For the purpose of determining the mass circulation of the LGM, we can suppose that one is interested instead, in determining the J_{ij} from observations of ^{14}C or the equivalent age. As noted above, $\tau_{14\text{C}}$ satisfies a very nonlinear forward equation, and as described by Wunsch (2002), it is advisable to use the underlying parent or parent and daughter tracers that satisfy a linear system.

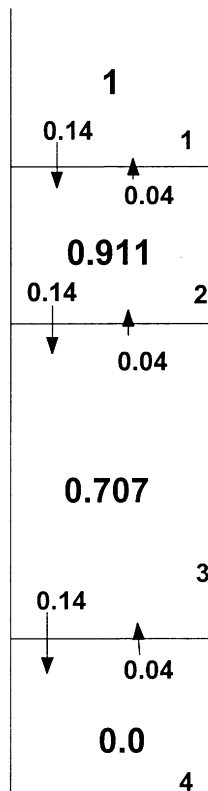


Fig. 10. One-dimensional model with steady-state ^{14}C distribution (1 at top, 0 at bottom), and corresponding J_{ij} , nominally in Sverdrups. The ^{14}C distribution, equivalent to the radiocarbon age, is used to infer the J_{ij} in the inverse calculation.

Consider, for maximum simplicity, a purely one-dimensional version of the current problem as depicted in Fig. 10. We suppose the ocean is a one-dimensional pipe flow, as depicted with two active interior boxes. The tracer has a decay constant λ_p and we suppose that the system is truly in a steady-state. For radiocarbon, we suppose only the parent distribution is known, abandoning the pretence that ^{14}N is measured. The two end boxes, at the top and bottom, are forced to known boundary properties, and hence the equations governing a steady-state tracer in the two interior boxes are of the form:

$$\begin{cases} C_1^p & -C_2^p & 0 & -C_2^p & C_3^p & 0 \\ 0 & C_2^p & -C_3^p & 0 & -C_3^p & C_4^p \\ 1 & -1 & 0 & -1 & 1 & 0 \\ 0 & 1 & -1 & 0 & -1 & 1 \end{cases} \begin{bmatrix} J_{12} \\ J_{23} \\ J_{34} \\ J_{21} \\ J_{32} \\ J_{43} \end{bmatrix} \\ = \begin{bmatrix} \lambda_p C_2^p V_2 \\ \lambda_p C_3^p V_3 \\ 0 \\ 0 \end{bmatrix}, \quad J_{ij} \geq 0, \quad (13)$$

with the first two equations corresponding to maintenance of a tracer steady-state, and the latter two representing mass conservation. The drastic assumptions of perfect data and a perfect model are being made, assumptions that greatly, but unrealistically, simplify the discussion.

An observed daughter tracer, if available, would provide two additional, generally linearly independent equations. For radiocarbon alone, there are four equations in six unknowns, plus the requirement that all $J_{ij} \geq 0$. This positivity requirement is important extra information, but requires the use of either linear programming or non-negative least-squares (see Wunsch, 1996, p. 300+ for a description and references.)

As a demonstration problem, we compute the parent distribution for a ^{14}C -like tracer, in which the equivalent ages in a steady-state are as given in Fig. 10. These values are inserted into the coefficient matrix in Eq. (13). In general therefore, there will be an infinite number of possible solutions for the J_{ij} unless some additional information is forthcoming. In the situation of Fig. 10 where the true solution is

$$\mathbf{J} = 10^5 \times [1.4, 1.4, 1.4, 0.4, 0.4, 0.4]^T,$$

a minimum 1-norm solution (minimum of $\sum_{ij} J_{ij}$ found by linear programming), is

$$\mathbf{J}_{\min} = 10^3 \times [9.42, 0.25, 0.25, 9.17, 0, 0]^T,$$

and which is significantly weaker in the lower part of the water column than the true solution, but nonetheless, exactly reproduces the “observed” tracer.

Legrand and Wunsch (1995) pointed out that stable, conserved tracer distributions alone do not permit inferences of the rates of ocean mass circulation. In the absence of information about production and destruction of the tracer, any circulation rate, including zero water movement can be rendered consistent with the data. Rate information for the modern ocean comes primarily from global measurements of geostrophic shear coupled with mass and tracer conservation rules. In the paleocean, the radiocarbon decay constant is one rate setter. Unsurprisingly, in view of the difficulties encountered in producing estimates of the modern circulation with a vastly greater data base, the radiocarbon data by themselves cannot produce a unique circulation. Some authors produce unique answers by arbitrarily reducing the degrees of freedom in the model. For example, by setting all of the “backflows”, $J_{21} = J_{32} = J_{43} = 0$, the system of equations becomes overdetermined, but the apparent definitive answer is then largely illusory, being wholly dependent upon the correctness of the flow and mixing assumptions.

As with any inverse problem however, even the most limited information can still be exploited to gain some understanding of the solution, and the present system is

no exception. We can, for example, use the linear programming methodology to find various bounds upon the J_{ij} . We first make the important inference that the available information does not provide any *upper* bound upon the J_{ij} . For example, it is readily seen that an infinite number of other perfect solutions to the problem is obtained by adding any positive multiple of $\mathbf{J}_n = [0.46, 0.61, 0.58, 0.05, 0.20, 0.18]^T$ to the above value of \mathbf{J}_{\min} . (This vector is in the nullspace of the coefficient matrix in (13). A second nullspace vector also exists.) An example of a large flux solution is $\mathbf{J} = 10^6 \times [10, 8.0, 10, 2.2, 0.2, 2.2]^T$.

In a two-dimensional situation, there would be an additional four J_{ij} for each box, and in three dimensions, up to eight additional unknown J_{ij} would appear. The information requirement for deducing a three-dimensional flow is forbidding unless one can take account of the dynamics linking the J_{ij} (the basis of state estimation, or data assimilation, with ocean general circulation models). To the degree that the boundary concentrations here, C_1^p, C_4^p , are unknown too, one requires even more data to determine the rate of circulation.

6.1. Three dimensions

Despite the apparent obstacles, consider now the three dimensional inverse problem, the analogue of the one-dimensional one just set up. The “data” are taken from the ^{14}C values of the forward calculation in Fig. 5. In this situation, the concentrations in the top layer function as a boundary condition, and no constraints are therefore written for these boxes. For each of the remaining 12 boxes, there is an equation for mass conservation and steady-state tracer distributions—for a total of 24 equations. Accounting for all neighbors, there are 46 unknown J_{ij} . The remaining information is that as before, $J_{ij} \geq 0$. As anticipated from the one-dimensional case, there is no upper bound on the J_{ij} . Seeking the minimum of $\sum_{ij} J_{ij}$ succeeds in producing a rather boring result (not shown) in which the only exchanges are very weak and completely vertical (no lateral circulation at all).

To explore the impact of an estimate of the western boundary current transport, an additional equation was written, forcing $J_{11,9} = 10$, $J_{9,11} = 0$ (exactly, and which is “correct”). The result is depicted in Table 1 and, as is consistent with results from inverse calculations of the present North Atlantic, is a purely local shift in the circulation, with no overall increase. One is forced to conclude that extant estimates of the LGM flow field are probably artifacts of over-simplified model assumptions.

In the present one-dimensional steady-state case, if the mass and radiocarbon constraints are combined with one more tracer, even a stable one, a uniquely determinable solution can be found (up to the suppressed noise elements). Thus a tracer like $\delta^{13}\text{C}$ could be

Table 1

J_{ij} , in Sverdrups, for the “forward” computation of the ^{14}C distribution (left three columns) and representing “truth”. Center three columns are the inversion for $\min(\sum_{ij}(J_{ij}))$. Third set of three columns are the solution for $\min(\sum_{ij}(J_{ij}))$, but subject to a forced western boundary current mass flux in the middle layer. Only non-zero elements are listed

i	j	J_{ij}	i	j	J_{ij}	i	j	J_{ij}
1	3	10	2	8	0.63	3	9	4.5
2	1	10	3	9	0.06	7	9	0.2
2	8	15	4	10	2.99	8	2	0.0
3	4	8	5	11	0.01	8	7	0.2
3	5	2	6	12	0.74	9	3	0.2
4	2	10	8	2	0.62	9	11	10
5	6	2	8	14	0.35	10	4	0.7
6	4	2	9	3	0.06	10	9	5.0
7	9	30	9	15	0.02	11	5	3.4
8	2	15	10	4	2.99	11	12	4.9
8	7	30	10	16	0.72	11	17	1.5
8	14	15	11	5	0.01	12	10	5.2
9	10	20	12	6	0.74	12	18	0.0
9	11	10	12	18	0.24	14	8	0.3
10	4	10	14	8	0.35	15	9	0.3
10	8	30	15	9	0.02	15	16	0.9
11	12	10	16	10	0.72	16	10	0.5
12	10	10	18	12	0.24	16	14	0.3
13	14	20				17	11	0.0
14	8	15				17	15	1.3
14	16	20				17	18	0.2
15	13	20				18	12	0.2
15	16	5						
16	15	5						
16	18	20						
17	15	20						
18	17	20						

used. The problem of a time-varying tracer, e.g., if the transient is on-going, can be solved by the methods of control theory (e.g., Wunsch, 1988b, 1996). Such a system is even less-well determined than is the steady-state one.

The major difficulty is the proliferation of data necessary to move to three dimensions. Even with the present over-simplified model, the existence of a total of 12 exchanges of each box with its neighboring boxes suggests the number of tracers that will eventually be necessary to determine the mass fluxes. Whether temperature and other fluxes can then also be determined, will depend upon the availability of a temperature proxy such as $\delta^{18}\text{O}$.

7. Discussion

The generic discussion here leads one back to the overall conclusion of Legrand and Wunsch (1995), but who lacked ^{14}C data: water mass volume distributions do not provide information on the rates of water

movement. The addition of radiocarbon with the known decay rate providing a renewal rate measure, and even with perfect values available in every sub-domain of the model, still provides only lower bounds upon the rate of the mass circulation. It is difficult to regard the result as supporting a conclusion that the LGM North Atlantic mass circulation was weakened; nothing can be said about the corresponding flux of heat or other scalar field.

It is useful therefore, to turn to other lines of evidence. As stated above, [Yu et al. \(1996\)](#) concluded that the circulation was, if anything, stronger during the LGM. They noted the apparent conflict with the inference of [Boyle and Keigwin \(1987\)](#) based upon cadmium distributions. But as those latter authors realized, the cadmium data are really a demonstration that the LGM equivalent of North Atlantic Deep Water migrated vertically higher into the water column, with an unknown mass flux. Increased flux of bottom water of circumpolar origin into the North Atlantic (e.g., [Adkins et al., 1998](#)) might well be regarded as an indicator of a strengthened mass circulation, not a weakened one. With NADW moving southward at a shallower depth and with an increased northward flux of very cold near-bottom water in the North Atlantic, the oceanic heat circulation could have been reduced, even in the presence of an overall increase in the mass fluxes. Whether such a situation actually obtained is probably only going to be determined with a global high resolution general circulation/biogeochemical model and more definitive surface conditions.

Inference of an increased mass circulation would appear to contradict the results of [Lynch-Stieglitz et al. \(1999\)](#) who used $\delta^{18}\text{O}$ measurements in cores on both sides of the Florida Straits to calculate the vertical shear in the Gulf Stream there during the LGM. The apparent shear was reduced compared to that of today, and using a level-of-no-motion at the seafloor, those authors concluded that the net mass transport during the LGM lay between 14 and 21 Sv, in contrast to modern values near 31 Sv. (The method used in practice for their modern result was actually somewhat different from the simple level-of-no-motion assumption described; J. Lynch-Stieglitz, pers. comm., 2001.)

If one examines modern hydrographic sections across the Florida Straits using a level-of-no-motion at the seafloor, they produce net transports of only about 24 Sv. It has thus been inferred (e.g., [Wunsch, 1996, p. 218](#)) that the actual mean velocity at the seafloor today is of order 20 cm/s to the north so as to account for the observed total transport and for consistency with the direct current meter measurements of [Schott et al. \(1988\)](#). The latter show very large near-bottom mean flows, even in the deepest part of the channel.

Whatever the details of the calculation, the real difficulty is that to calculate the actual transport during the LGM, one must have an estimate of the reference

level velocity. Unfortunately, as is well-known in the conventional dynamic method, there is no information available about the reference level velocity from the geostrophic shear alone: additional information is required.¹ In more general terms, the total flow through the Florida Straits is set by forces acting over the entire ocean, and the simplest interpretation of the [Lynch-Stieglitz et al. \(1999\)](#) data is that although there might have been a reduced baroclinic shear in the Florida Straits during the LGM, exactly as in the modern problem, one cannot infer the absolute geostrophic velocity or transports from an isolated section. With a strengthened wind-system, the total transport was likely to be larger than today, rather than smaller.

What did happen in the North Atlantic during the LGM? Data support the hypothesis that North Atlantic Deep Water migrated vertically, and unsurprisingly, given the likely changed surface boundary conditions, had somewhat different characteristics than today. Perhaps the baroclinic shear of the Florida Current was slightly reduced then. More high radiocarbon-age (low- ^{14}C concentration) abyssal water was present further north. Otherwise, the mass flux of the LGM-NADW remains unconstrained. It is possible that the North Atlantic meridional overturning circulation became more like that seen in the South Pacific today (e.g., [Wijffels et al., 2001](#)), with an intensified inflow, at the bottom, of southern hemisphere water, a stronger Gulf Stream system, and a greater southward flux of an intermediate depth water perhaps worth labeling as Glacial Intermediate Water rather than as NADW (cf. [Boyle, 1995](#)). As with the modern Pacific Ocean, the poleward heat flux of such a system is comparatively modest compared to the strong underlying mass flux, simply because the temperature differences involved in the circulation are reduced compared to the present-day North Atlantic (the South Pacific meridional overturning mass circulation is roughly twice that for the North Atlantic, yet it carries a smaller temperature flux).

What would be the effect on the circulation of regionally intensified mixing, primarily at ocean boundaries, whether from increased tides or winds? Answering such a question is not something that can be done by pure thought; one must carefully integrate the equations of motion with adequate resolution.

Determining the LGM ocean circulation is no simpler than determining the modern one. One must carefully separate discussions of the mass circulation from that of heat and salt (or freshwater equivalent) and of nutrients, oxygen and carbon. There is no reason to expect that

¹In principle, the dynamic method can produce the absolute velocity if extremely accurate three dimensional density distributions are available, using Needler's formula and related expressions such as the β -spiral; see [Wunsch \(1996\)](#). In practice, inverse methods are used to make the inferences in the presence of the inevitable noise.

these circulations are ever identical, and the modern system shows how different they can be; the semantic distinctions must be maintained. Radiocarbon ages and geostrophic shears can be used to make inferences about mass fluxes, but these inferences will depend directly upon the realism of the underlying model. In particular, the three-dimensionality is essential, and given the long time constants for adjustment, one must be alert to the possibility that the system is not in steady-state, either in terms of adjustment to changing tracer boundary conditions, or to a changing flow field, or both. Given the dependence of all elements of the circulation on the wind field, determining its strength and pattern during the LGM has to be a very high priority.

No one would attempt to calculate the absolute transport in the modern system from isolated sections depicting geostrophic shear, nor from water mass volumes alone. Oceanographers are moving towards estimating the circulation from quantitative combinations of dynamical models and observations of all kinds, using inverse and state estimation methods (Wunsch, 1996; Stammer et al., 2002). There is every reason to believe that useful state estimates of the LGM ocean will require a similar approach, as well as a much larger data base than exists now. In the absence of basin-distributed values of geostrophic shear, the simple inverse problems described above show that a data base permitting calculations of horizontal and vertical gradients of multiple tracers will be both necessary and adequate to make quantitative inferences about flux rates. The effort needs to be a global one: in regional box models, as used here, the freedom to postulate tracer concentration changes at depth on interior open boundaries renders all conclusions subject to error and controversy. A global box model removes much of this arbitrariness, with the surface concentrations/fluxes then being the only unconstrained boundary conditions. Coupled with continued attempts to determine more, and more widespread, rate-setting, tracers and paleo-shear measurements, one should ultimately be able to determine the mass circulation.

Acknowledgements

I thank P. Huybers, J. Adkins and R. Toggweiler for useful comments (not necessarily implying agreement).

Appendix A. Age relations

For a solid in which particle diffusion is negligible, the parent/daughter tracer equations become

$$\frac{\partial C_p(t)}{\partial t} = -\lambda C_p(t), \quad (\text{A.1})$$

$$\frac{\partial C_d(t)}{\partial t} = \lambda_p C_p(t). \quad (\text{A.2})$$

If the parent has initial concentration $C_p(0)$, the solutions are

$$C_p(t) = C_p(0)e^{-\lambda_p t}, \quad C_d(t) = C_p(0)(1 - e^{-\lambda_p t}). \quad (\text{A.3})$$

Then one has immediately from

$$\tau_p(t, \lambda_p) = \frac{1}{\lambda_p} \ln \left(1 + \frac{[C_d(t)]}{[C_p(t)]} \right) = t. \quad (\text{A.4})$$

Also,

$$\tau'_p(t, \lambda_p) = -\frac{1}{\lambda_p} \ln \left[\frac{C_p(t)}{C_p(0)} \right] = t \quad (\text{A.5})$$

which gives the time wholly in terms of the initial and current concentrations of the parent.

In a system with advection and diffusion, $\tau_p \neq \tau'_p$, since the equation governing τ_p is very different from that governing C_p . In addition, the corresponding different boundary conditions will have a major influence on the final values. In using (A.5) in a system with a spatial variation, $C_p(0)$ would be chosen as the nominal surface value at $t = 0$.

A comparison of the two tracer ages in a simple configuration may be useful. Consider (Wunsch, 2002) the steady-state advective diffusive balance, which replaces (A.1, A.2),

$$w \frac{\partial C_p}{\partial z} - \kappa \frac{\partial^2 C_p}{\partial z^2} = -\lambda_p C_p, \quad (\text{A.6})$$

$$w \frac{\partial C_d}{\partial z} - \kappa \frac{\partial^2 C_d}{\partial z^2} = \lambda_p C_p \quad (\text{A.7})$$

with the surface concentrations $C_p(z = 0)$, and $C_d(z = 0) (= 0)$, as with the tritium–helium pair. Then the parent concentration is

$$C_p(z) = C_p(0) \exp \left(\frac{zw}{2\kappa} \left[1 + \sqrt{1 + 4\lambda_p \kappa / w^2} \right] \right), \quad z < 0 \quad (\text{A.8})$$

and which produces

$$\tau'_p = \frac{|z|w}{2\lambda_p \kappa} \left[1 + \sqrt{1 + 4\lambda_p \kappa / w^2} \right]. \quad (\text{A.9})$$

To find τ_p one must find the concentration, $C_d(z)$; the result is (Wunsch, 2002, Eq. (43)),

$$\tau_p = \frac{|z|w}{2\lambda_p \kappa} \left[\sqrt{1 + 4\lambda_p \kappa / w^2} - 1 \right]. \quad (\text{A.10})$$

Taking modern values, $\kappa = 10^{-4} \text{ m}^2/\text{s}$, $w = 10^{-7} \text{ m/s}$, and $\lambda_p = 1/8500 \text{ y} \approx \lambda_p = 3.7 \times 10^{-12}$, one finds for $z = -2000 \text{ m}$, $\tau = 490 \text{ y}$, $\tau' = 2219 \text{ y}$. A change in λ_p would change the values.

Appendix B. Intrinsic time scales

The state transition matrix \mathbf{A} (omitting subscript p) is full-rank and the eigenvalue/eigenvector problem,

$$\mathbf{A}\mathbf{g}_i = l_i\mathbf{g}_i, \quad (\text{B.1})$$

produces M unit length vectors \mathbf{g}_i which are a spanning (complete) set, but they are *not* orthogonal (\mathbf{A} is not symmetric), and the l_i need not be real. The matrix $\mathbf{G} = \{\mathbf{g}_1, \mathbf{g}_2, \dots, \mathbf{g}_M\}$ can be used to diagonalize \mathbf{A} :

$$\mathbf{G}^{-1}\mathbf{A}\mathbf{G} = \mathbf{L}, \quad (\text{B.2})$$

where $\mathbf{L} = \text{diag}(l_i)$. We can use this result (e.g., Brogan, 1985) to re-write Eq. (3) as

$$\mathbf{G}^{-1}\mathbf{x}(t+1) = \mathbf{G}^{-1}\mathbf{A}\mathbf{G}\mathbf{G}^{-1}\mathbf{x}(t) + \mathbf{G}^{-1}\mathbf{q}(t) \quad (\text{B.3})$$

or

$$\mathbf{z}(t+1) = \mathbf{L}\mathbf{z}(t) + \mathbf{q}'(t) \quad (\text{B.4})$$

$$\mathbf{z}(t) = \mathbf{G}^{-1}\mathbf{x}(t), \quad \mathbf{L} = \mathbf{G}^{-1}\mathbf{A}\mathbf{G}, \quad \mathbf{q}'(t) = \mathbf{G}^{-1}\mathbf{q}(t) \quad (\text{B.5})$$

that is each element of $\mathbf{z}(t)$ evolves independently of every other element, in the form:

$$z_i(t+1) = l_i z_i(t) + q'_i(t). \quad (\text{B.6})$$

In an initial value problem, $q'_i = 0$, $z_i(0)$ known, one has immediately,

$$z_i(t) = l_i^t z_i(0) = z_i(0)e^{t \log(l_i)} = z_i(0)e^{-t/T_i}. \quad (\text{B.7})$$

Stability requires $|l_i| \leq 1$, and it is readily confirmed to be true in the problems formulated here. The values of $T_i = 1/\log(|l_i|)$ are in Table 2 in years; they summarize the time constants of decay present in the model.

Table 2

Time constants, T_i in years for a stable tracer, $\lambda = 0$. Repeated values at 10.8 yr correspond to two complex, conjugate, values with the same real part. All others are real

∞	51.3	10.8	10.8	6.6	4.3	1.9	1.4	1.0	0.3
	0.3	0.29	0.21	0.15	0.07	0.06	0.05	0.01	

One mode, with largest absolute, and real, eigenvalue, $l_1 = 1$, is everywhere a constant: if excited by an initial condition, this mode never decays, as it is physically sensible. Each element $z_i(t)$ maps back onto the full physical space by

$$\xi_j(t) = \mathbf{G} \begin{bmatrix} 0 \\ 0 \\ \cdot \\ z_j(t) \\ \cdot \\ 0 \end{bmatrix} = z_j(t)\mathbf{g}_j. \quad (\text{B.8})$$

The \mathbf{g}_j corresponding to the very short time scales tend to be localized in small boxes, in which the entire

contents can be replaced by the J_{ij} very quickly. Those corresponding to time scales longer than about 1 year describe large-scale distributions involving most of the three dimensional region. Any initial disturbance exciting \mathbf{g}_1 remains forever within the system. The second slowest mode requires about 50 years to decay to an amplitude of e^{-1} of its initial value and remnants would be present for a considerably longer time. Because the \mathbf{g}_i are non-orthogonal, the expansion coefficients for an arbitrary initial condition have to be found by solving a set of linear simultaneous equations.

References

- Adkins, J.F., Cheng, H., Boyle, E.A., Druffel, E.R.M., Edwards, R.L., 1998. Deep-sea coral evidence for rapid change in ventilation of the deep North Atlantic 15,400 years ago. *Science* 280, 725–728.
- Bard, E., 1988. Correction of accelerator mass spectrometry ^{14}C ages measured in planktonic foraminifera: paleoceanographic implications. *Paleoceanography* 3, 635–645.
- Boyle, E.A., 1995. Last-glacial maximum North Atlantic deep water: on, off or somewhere in-between? *Philosophical Transactions of the Royal Society B* 348, 243–253.
- Boyle, E.A., Keigwin, L.D., 1987. Deep circulation of the North Atlantic over the last 20,000 years: geochemical evidence. *Science* 218, 784–787.
- Bradley, R.S., 1999. *Paleoclimatology: Reconstructing Climates of the Quaternary*. Harcourt/Academic, San Diego, 613 pp.
- Broecker, W.S., Peng, T.H., 1982. *Tracers in the Sea*. Eldigio Press, Palisades, NY, 690 pp.
- Broecker, W.S., Peng, T.-H., Trubore, S., Bonani, G., Wolfli, W., 1990. The distribution of radiocarbon in the glacial ocean. *Global Biogeochemical Cycles* 4, 103–117.
- Broecker, W.S., Virgilio, A., Peng, T.-H., 1991. Radiocarbon age of waters in the deep Atlantic revisited. *Geophysical Research Letters* 18, 1–3.
- Brogan, W.L., 1985. *Modern Control Theory*, 2nd Edition. Prentice-Hall/Quantum, Englewood Cliffs, NJ, 393 pp.
- Bryden, H.L., Imawaki, S., 2001. Ocean heat transport. In: Siedler, G., Church, J., Gould, J. (Eds.), *Ocean Circulation and Climate*. Academic Press, San Diego, pp. 455–474.
- Crowley, T.J., North, G.R., 1991. *Paleoclimatology*. Oxford, New York, 339 pp.
- Ganachaud, A., Wunsch, C., 2000. Oceanic meridional overturning circulation, mixing, bottom water formation and heat transport. *Nature* 408, 453–457.
- Ganachaud, A., Wunsch, C., 2002. Oceanic nutrient and oxygen fluxes during the World Ocean Circulation Experiment and bounds on export production. *Global Biogeochemical Cycles*, 16(4), 1057, DOI: 10.1029/2000GB00133.
- Gray, S.L., Haine, T.W.N., 2001. Constraining a North Atlantic Ocean general circulation model with chlorofluorocarbon observations. *Journal of Physical Oceanography* 31, 1157–1181.
- Huang, R.X., 1999. Mixing and energetics of the oceanic thermohaline circulation. *Journal of Physical Oceanography* 29, 272–276.
- Huang, R.X., Schmitt, R.W., 1993. The Goldsbrough-Stommel circulation of the world oceans. *Journal of Physical Oceanography* 23, 1277–1284.
- Jenkins, W.J., 1988. The use of anthropogenic tritium and helium-3 to study subtropical gyre ventilation and circulation. *Philosophical Transactions of the Royal Society of London A* 325, 43–61.

- Ledwell, J.R., Montgomery, E.T., Polzin, K.L., St. Laurent, L.C., Schmitt, R.W., Toole, J.M., 2000. Evidence for enhanced mixing over rough topography in the abyssal ocean. *Nature* 403, 179–182.
- LeGrand, P., Wunsch, C., 1995. Constraints from paleo-tracer data on the North Atlantic circulation during the last glacial maximum. *Paleoceanography* 10, 1011–1045.
- Lynch-Stieglitz, W., Curry, B., Slowey, H., 1999. Weaker Gulf Stream in the Florida Straits during the Last Glacial Maximum. *Nature* 402, 644–648.
- Mémery, L., Wunsch, C., 1990. Constraining the North Atlantic circulation with tritium data. *Journal of Geophysical Research* 95, 5229–5256.
- Munk, W., Wunsch, C., 1998. Abyssal recipes II: energetics of tidal and wind mixing. *Deep-Sea Research I* 45, 1976–2009.
- Paparella, F., Young, W.R., 2002. Horizontal convection is non-turbulent. *Journal of Fluid Mechanics* 466, 205–214.
- Schott, F.A., Lee, T.N., Zantopp, R., 1988. Variability of structure and transport of the Florida Current in the period range of days to seasonal. *Journal of Physical Oceanography* 18, 1209–1230.
- Sikes, E.L., Samson, C.R., Guilderson, T.P., Howard, W.R., 2000. Old radiocarbon ages in the southwest Pacific Ocean during the last glacial period and deglaciation. *Nature* 405, 555–559.
- Stammer, D., C. Wunsch, R. Giering, C. Eckert, P. Heimbach, C. Hill, J. Marotzke, J. Marshall, 2002. The global ocean state during 1992–1997, estimated from ocean observations and a general circulation model. Part I. Methodology and estimated state. *Journal of Geophysical Research*, DOI: 10.1029/2001JC000888.
- Stommel, H., 1961. Thermohaline convection with two stable regimes of flow. *Tellus* 13, 224–230.
- Stommel, H., Rooth, C., 1968. On the interaction of gravitational and dynamic forcing in simple circulation models. *Deep-Sea Research* 15A, 165–170.
- Wijffels, S.E., Toole, J.M., Davis, R., 2001. Revisiting the South Pacific subtropical circulation: a synthesis of World Ocean Circulation experiment observations along 32°S. *Journal of Geophysical Research* 106, 19481–19513.
- Wunsch, C., 1988a. Eclectic modelling of the North Atlantic. II. Transient tracers and the ventilation of the eastern basin thermocline. *Philosophical Transactions of the Royal Society A* 325, 201–236.
- Wunsch, C., 1988b. Transient tracers as a problem in control theory. *Journal of Geophysical Research* 93, 8099–8110.
- Wunsch, C., 1996. *The Ocean Circulation Inverse Problem*. Cambridge University Press, Cambridge, 437 pp.
- Wunsch, C., 2002. Oceanic age and transient tracers. Analytical and numerical solutions. *Journal of Geophysical Research* 107(C6), 10.1029/2001JC000797.
- Yu, E.-F., François, R., Bacon, M.P., 1996. Similar rates of modern and last-glacial ocean thermohaline circulation inferred from radiochemical data. *Nature* 379, 689–694.